MOVEMENT OF A FLUORESCENT LIPID LABEL FROM A LABELED ERYTHROCYTE MEMBRANE TO AN UNLABELED ERYTHROCYTE MEMBRANE FOLLOWING ELECTRIC-FIELD-INDUCED FUSION

ARTHUR E. SOWERS
American Red Cross Laboratories, Bethesda, Maryland 20814

ABSTRACT A short burst of electric field pulses was used to induce nearly simultaneous fusion among 50% or more of a population composed of unlabeled erythrocytes and erythrocytes labeled with the fluorescent lipid analogue DiI (1,1',-dihexadecyl-3,3,3'',3'-tetra-methylindo carbocyanine perchlorate). Fusion products that ended in an hourglass shape were selected for analysis. The net movement of the label from the labeled membrane to the adjacent unlabeled membrane in each of the hourglass-shaped fusion products was recorded by micrography at various known times after the fusion took place, but before equilibrium was achieved. The lateral concentration gradients were measured by densitometry and compared with predictions based on Huang's model (Huang, H.-W., 1973, *J. Theor. Biol.*, 40:11–17) for lateral diffusion on a spherical membrane. The average lateral diffusion coefficients, 3.8 and 8.1 $\times 10^{-9}$ cm^2/s in pH 7.4 isotonic phosphate buffer at 23–25°C and 35–37°C, respectively, compare very favorably with the results of three published photobleaching studies of the lateral diffusion of DiI in erythrocyte membranes. While the fusion approach to measuring lateral diffusion is not new, it has not enjoyed widespread use because of the uncertainty in the degree of fusion synchrony and low fusion yield. This study shows that the use of pulsed electric fields to induce synchronous fusion is a promising approach to overcome both of these drawbacks and yield results comparable to those obtainable by the photobleaching approach.

INTRODUCTION

The lateral diffusion coefficient for membrane components has been previously measured by following the movement of labeled components from labeled membranes to unlabeled membranes after the two membranes are fused (1–4). This approach has been recently given the acronym FRAF, for Fluorescence Redistribution After Fusion (4). In these studies, fusion was induced by creating chemical (polyethylene glycol in references 2, 4) or biological (Sendai virus in references 1, 2, 3) conditions favorable for fusion to occur. However, the low frequency of fusion requires a search of many membranes to locate a few fused membranes. Also, since discovery of these fused membranes is likely to occur at a significant amount of time after the fusion event, there will be an appreciable amount of uncertainty in the estimation of how far into the past fusion took place, even if back extrapolation is used. The recent discovery that both a high-fusion yield and fusion can be induced in many membranes simultaneously, or nearly simultaneously, in a given preparation by electric field pulses (for reviews see references 5, 6) offers a way around these two problems.

This paper describes the principles, the required experimental setup, and the procedure we followed in using electric field induced fusion in the FRAF approach to measure the lateral-diffusion coefficient for DiI in human erythrocyte membranes in isotonic phosphate buffer (pH 7.4). Portions of this work have been reported in preliminary form (7).

METHODS

Human whole blood collected in plastic bags containing a citrate-phosphate-dextrose-adenine mixture was obtained from the Washington, DC American Red Cross Regional Blood Services. Packed red cells were obtained by centrifugation at 300 *g* for 10 min. Packed red cells were resuspended and were washed at least once in isotonic sodium phosphate buffer (pH 7.4), at 0–4°C. Red cells were labeled with the fluorescent dye DiI(C-16) as follows: Pelleted red cells were resuspended at the rate of 0.5 ml per 4.45 ml of labeling buffer (100 mM sucrose, 20 mM sodium phosphate, pH 7.4). A quantity (50 μl) of DiI in ethanol (3.5 mg/ml) was added to the red cell suspension and incubated at 37°C for 30 min (labeling was much less extensive and less homogeneous if higher phosphate concentrations were used). Red cells were then pelleted and washed two times in isotonic pH 7.4 buffer at room temperature (23–25°C). DiI was obtained from Molecular Probes (Junction City, OR). All other chemicals were obtained from Sigma Chemical Co. (St. Louis, MO).

Working red cell suspensions were made by diluting labeled and unlabeled pellets with 15–20 vol of isotonic phosphate buffer (pH 7.4). Working labeled membrane suspensions were mixed with working unlabeled membrane suspensions in the ratio of ~1:7, and added to the fusion

chamber (Fig. 1) from one of the two sides to result in the filling of the chamber by capillary wicking. An extra quantity of the mixed membrane suspension was added to both sides to make reservoir pools. The fusion chamber was then inverted and fastened to the fusion slide frame (Fig. 1) with tape.

Wire (no. 22 gauge tinned-copper) electrodes were immersed to a depth of ~1 mm in each reservoir pool. The remaining components of the overall setup were as follows. The fusion slide, which carried the fusion chamber, was then placed on the stage of laboratory microscope (model 16; Carl Zeiss, Inc., Thornwood, NY) equipped with a 35mm camera having a motor-driven film advance controlled by a Zeiss MC 63 shutter control, a 100 W Zeiss epifluorescence illuminator, a Zeiss FITC filter set, and an oil 100× plan achro 1.24 NA objective lens (Carl Zeiss, Inc.). After a wait of 2–3 min to allow red cells to fall and pack close enough to touch each other in a nearly continuous monolayer of cells, fusion was induced by applying a train of pulses from a very simple circuit (Fig. 1) composed of a mercury-wetted relay pulser which alternately cycled a capacitor, C_2, betwen a charging circuit (involving a series connection with a (DC) electrophoresis-type power supply) and a discharging circuit involving a series connection with the fusion chamber electrodes. Since adjustment of the concentration of red cells in the suspension led to different final cell densities in the cell monolayer formed after red cell sedimentation, the ratio of hourglass-shaped doublet fusion products to polysphere fusion products could be controlled. The circuit was made to alternate between these two circuits by driving the relay coil with a current from the 60 Hz alternating current (AC) lines. The length, width, and height of the fusion chamber were ~2.0, 1.5, and 0.075 mm respectively. Separate experiments (Sowers, A. E., manuscript accepted for publication) with a storage screen oscilloscope showed optimum or nearly optimum fusion efficiency with a capacitor (C_2) value (0.01 μf) such that the decay half time of the pulses, the major critical variable in electric field-induced fusion in these membranes, which were delivered to the conductive suspension was ~0.3–0.6 ms. Between 700–1,000 V applied to the input terminals of this circuit was found to be the voltage range needed to give optimum fusion.

A delay timer controlled the time interval during which the train of pulses was delivered to the membranes and medium. Simultaneous with this train of pulses was a note from an audio beeper. A cassette deck recorded the audio note that signaled the interval during which pulses were applied (and fusion occurred) and, after various time intervals, recorded the camera shutter noises. Simultaneous fusion and significant fusion yields were apparent with a pulse train composed of ~40–60 pulses. During playback of the cassette recorder human reaction time was estimated to contribute less than about ±0.5 s error. Thus the interval, t, between the moment of fusion and the moment each micrograph was made, could be accurately determined. The associated time constant, T_c, for the gradient in each micrograph is also needed to calculate the lateral diffusion coefficient. This was accomplished as follows.

Micrographs were made with 1/4 or 1/2 s exposures on 35 mm color film (VR-1000, Kodak Laboratory and Specialty Chemicals, Rochester, NY), processed with the Unicolor K2 chemistry kit for the Kodak C-22 process according to instructions. Black and white positive images (Fig. 2) were printed on Kodak commercial film (4127) or Kodak royal pan (4141) (Kodak Laboratory and Specialty Chemicals) from the color negative images on the developed VR-1000 film, and scanned along a line passing through both poles of the image of the hourglass-shaped fusion products (Fig. 3) using a one-dimensional gel scanner (Quick Scan R + D, Helena Laboratories, Beaumont, TX) in the percent transmission mode (separate tests were made to ensure that all exposures were made on the linear portion of the characteristic curves of the emulsions used). Upon fusion, membranes became quickly converted from the two-membrane two-sphere configuration to a single membrane with the hourglass configuration (Fig. 2). To avoid the need for an overlap correction for the resolution profile of the lens, and a trigonometric correction for the fluorescence intensity of a point on a luminous plane with angles of incidence that would change markedly along a scan line from one pole to the other pole of the hourglass-shaped fusion product,

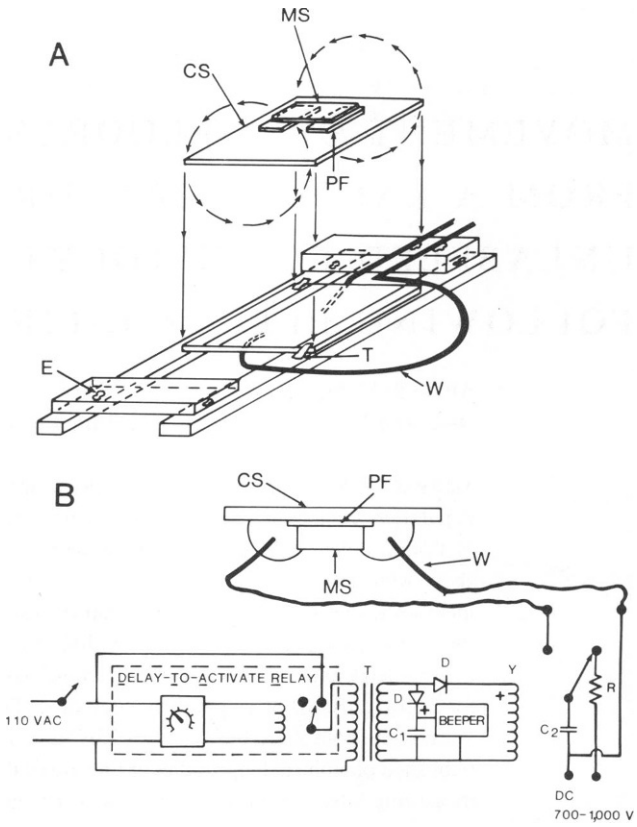

FIGURE 1 Fusion chamber, fusion slide, and circuit for inducing pulses: (*a*) Fusion slide composed of fusion chamber and fusion slide frame. Fusion chamber is bounded on upper and lower sides by a 22 × 22 mm coverslip, *CS*, and microslide, *MS*, (2.0 mm wide, 10 mm long, and 1.0 mm thick) cut from a standard 25 × 75 × 1 mm glass microscope slide. The chamber is bounded on the two sides by single sheets of parafilm ~ 2 × 2 mm and with edges separated from each other by ~1.5 mm to form a rectangular space 2.0 mm long, 1.5 mm wide, and ~0.075 mm high. The parafilm holds the *CS* to the *MS* after brief compression in a dry-mounting press set for 65°C. Wire electrodes (No. 22 gauge, tinned copper), *W*, are bent and positioned until immersed ~1.0 mm into each fluid reservoir (see text) on each side of the fusion chamber. The fusion chamber is turned upside down and fastened to the fusion slide frame with tape, *T*, to make the complete fusion slide. The fusion slide frame is made from two 5 × 75 mm and two 5 × 25 mm strips cut from a standard microscope slide with a diamond scribe and cemented together with epoxy cement, *E*. (*b*) Circuit used to generate a train of exponentially decaying pulses for inducing fusion. Line switch connects power to the delay-to-activate relay and primary of step-down transformer, *T*, having a 12.6 V secondary. After a delay of 0.7–1.0 s the delay relay removes power from the transformer. Diodes, *D*, rectify the transformer secondary alternating current to pulsating direct current, which is either filtered by C_1 (100 μf), and fed to the audio note generating device (beeper) or fed, unfiltered, to the coil of the mercury-wetted relay, *Y* (Clare HGSM 5009 or equivalent; General Instrument Corp., Clare Div., Chicago, IL), which drives the armature (arrow) from the resting position on the right contact to the left contact on each pulse. This causes capacitor C_2 to discharge through the membrane and membrane-containing medium load in the fusion chamber. After the relay pulse, the armature returns to the resting position, which allows the capacitor to be recharged through a resistor ($10^3\ \Omega$) that prevents an excessive current from passing through the relay contacts.

two locations on the scans of the positive images on film were chosen for fluorescence intensity measurement where the membrane was perpendicular to the optical axis. These locations were on the two equatorial meridians that coincided with the maximum diameter of each bulb of the hourglass (Fig. 3 *a*). The height of the scan line (H_L) at the chosen point of the originally labeled membrane and the height of the scan line (H_U) at the chosen point on the originally unlabeled membrane were recorded. Since the gradient predicted by Huang (8) is always symmetrical about the midpoint of the gradient, comparing either H_L or H_U to the center of the gradient, H_M, is equivalent. Furthermore, use of either is valid for comparison with Huang's model as long as the equilibrium concentrations in the measured membrane or the model membrane are normalized to each other. The equilibrium concentration was set to 1.0 in the computer program used to reproduce Huang's model and measures of H_L were normalized to this by using measures of H_L and H_U and calculating H_L (norm) = $2H_L/(H_L + H_U)$. Comparison of the normalized concentration, H_L (norm), for the measured membrane with Huang's model required that an analogous point that was equivalent to the measured location on the hourglass-shaped membrane be located on the model. This was accomplished by considering that at any given time the concentration at any location on the hourglass membrane (Fig. 3 *b*) should be, to a first approximation, comparable to an analogous location of the model, (Fig. 3) at a comparable proportional circumferential distance from either of the two respective poles.

Averages of measurements of the total pole-to-pole membrane fusion product length, S, and lumen diameters, L, and the locations on the hourglass-shaped membranes were H_L and H_U were measured (Fig. 3) indicated that the concentration at $\theta = 60°$, 120°C, i.e., $C(\pm 0.5, AT_c)$, on Huang's model (Fig. 4, reference 8) would correspond to the locations where H_L and H_U, respectively, were measured on the hourglass-shaped fusion product membrane. Plots from Huang's model of the relative concentration decreases at $\theta = 60°$ on the originally labeled side and of the relative concentration increase at $\theta = 120°$ on the originally unlabeled side are shown in Fig. 4 as a function of the number, A, of the time constants, T_c, (i.e., the product $A \cdot T_c$) after release. Values of t and values of A associated with the value of H_L (norm) for each micrographed membrane were plotted with t on the ordinate and A on the abscissa so that the slope of a regression line for all points would represent the average time constant, T_c, for the relaxation process. A Marquardt-Levenberg least-square fit (using a reiterative process forcing a fit through the origin) was obtained using the VAX RS/1 (Digital Equipment Corp., Marlboro, MA) software package. Since peak-to-peak noise on the measured gradients was on the order of 10% of the full scale values, gradients were analyzed only if the corresponding value for A was >0.15 or <2.0 (Fig. 4).

All gradients and measurements of the lumen diameter, L, and the pole-to-pole length, S, of each hourglass fusion product were made from sequences of micrographs having $8 < t < 71$ s after the initiation of the pulse train that induced fusion. Sequences contained 2 to 5 (mode = 4) micrographs of the same field of membranes that showed a progression in the lateral diffusion of the label from the originally labled side to the originally unlabeled side of the fused membranes. The average radius, R, for the equivalent sphere of Huang's model was calculated from average measurements of S, L, and the location of H_L (Fig. 3). The lateral diffusion coefficient was calculated from the equation $D = R^2/2T_c$. To obtain measurements at 35–37°C, the microscope stage was surrounded by a plastic tent into which warmed air was pumped and circulated. The temperature was monitored with a dial gauge.

RESULTS

Fluorescent discocytes and echinocytes were observed to convert to spherical shapes during the interval in which the train of fusion-inducing pulses were applied to the membranes in the fusion chamber. Observation of the same process in phase optics or brightfield optics revealed that hemoglobin was often lost from the cytoplasmic compartment and gained in the background (Sowers, A. E., manuscript accepted for publication). This is consistent with other reports of electric field induced pores and increases in permeability (see references 5, 6 for review).

Gradients and physical dimensions S and L from a total of 70 membrane micrographs made over time intervals of $8 < t < 71$ s for 23–25°C and from a total of 16 membranes over time intervals of $7 < t < 16$ s for 35–37°C were analyzed. Fig. 5 shows that a distinct and significant lumen appeared before the first micrograph was made of each hourglass fusion-product membranes. Thus, for most fusion events, substantial progress was made in achieving the final geometry in a time interval which is comparatively short (i.e., <8 s), compared to the entire interval (up to 71 s) over which micrographs of the lateral diffusion process were made. The average pole-to-pole length, S, of the fusion product membranes was 13.4 μm. The average lumen diameter, L, was 5.6 μm. The average radius, R, of the single equivalent sphere was 5.06 μm. The values of A and t associated with each membrane micrograph were plotted and a reiterative straight-line fit through the origin were made for both the 23–25°C (Fig. 6) and the 35–37°C (not shown) data. The time constants, based on the slope through the origins were 33.3 and 15.8 s, respectively.

DISCUSSION

Our average value (Table I) for the lateral diffusion coefficient for DiI in human erythrocyte membranes agrees very favorably in magnitude, and temperature dependence with comparable average values from three other laboratories (9, 10, 11). The lateral diffusion coefficient, D = 3.8 and 8.1 $\times$ 10^{-9} cm^2/s at 23–25°C and 35–37°C, respectively in isotonic phosphate buffer (pH 7.4). Densitometer scans frequently yielded values for measured H_L that were higher than those expected from Huang's model (note in Fig. 2 *e, f,* and *g,* the slightly greater height of the curves at the midpoint, and a markedly greater height at the left and right edges as compared to the neighborhoods of these points). This may have come about for two reasons. First, because the circumferential groove geometry at the constriction of the hourglass fusion product causes a slightly greater intensity to be recorded at the center of the gradient for the same reason that the edges of the membrane are slightly brighter than the center—the membrane is more parallel to the optical axis at these points and thus a greater effective dye concentration is detected per unit solid angle. Second, the plane of the constriction in the hourglass fusion product, being perpendicular to the gradient, may also restrict lateral diffusion. Hence, comparatively more labeled molecules will pile up on the originally labeled side of the constriction in the vicinity of the constriction because the labeled molecules approach necessarily smaller areas before they reach the constriction. This results in higher

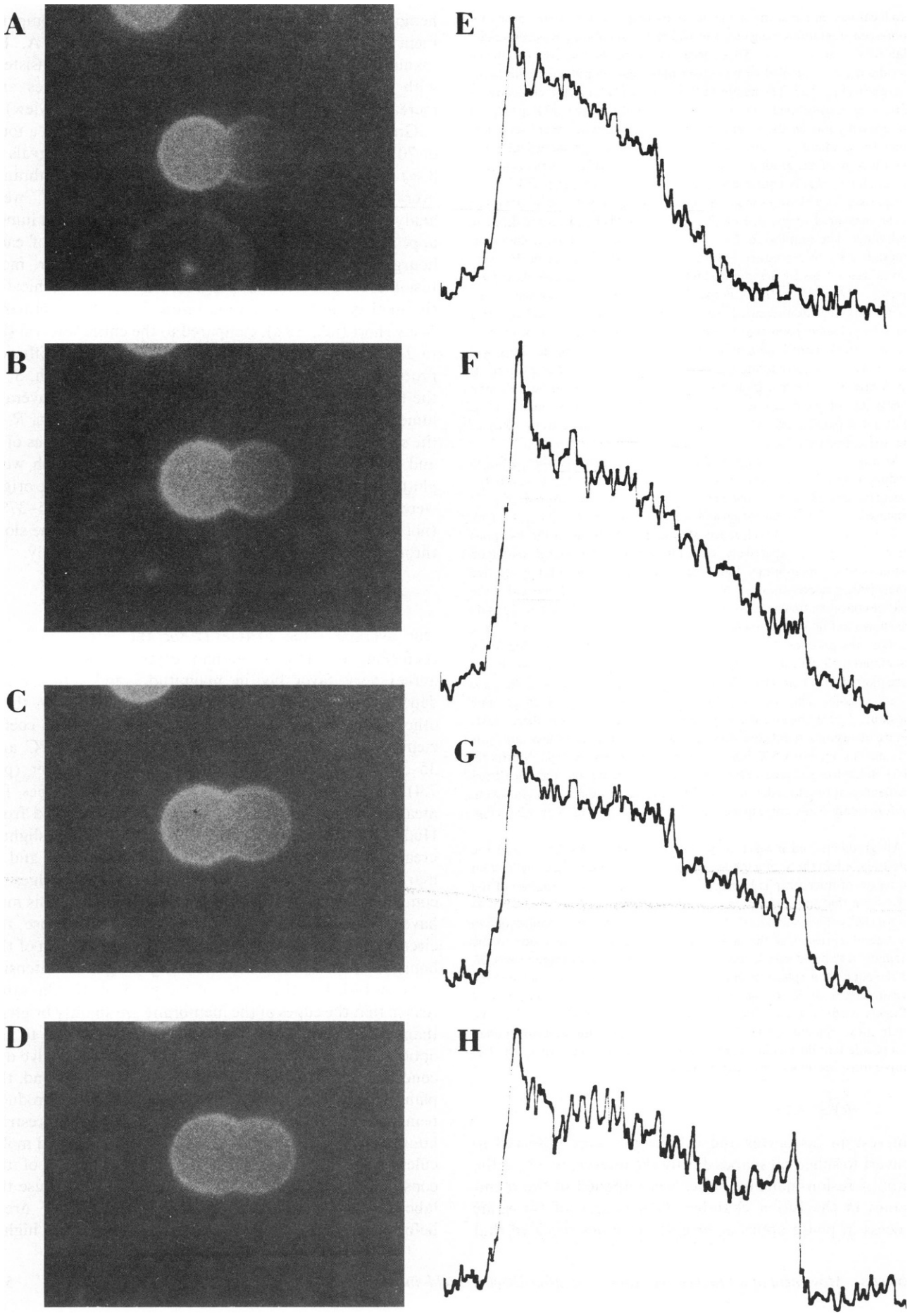
A
B
C
D
E
F
G
H

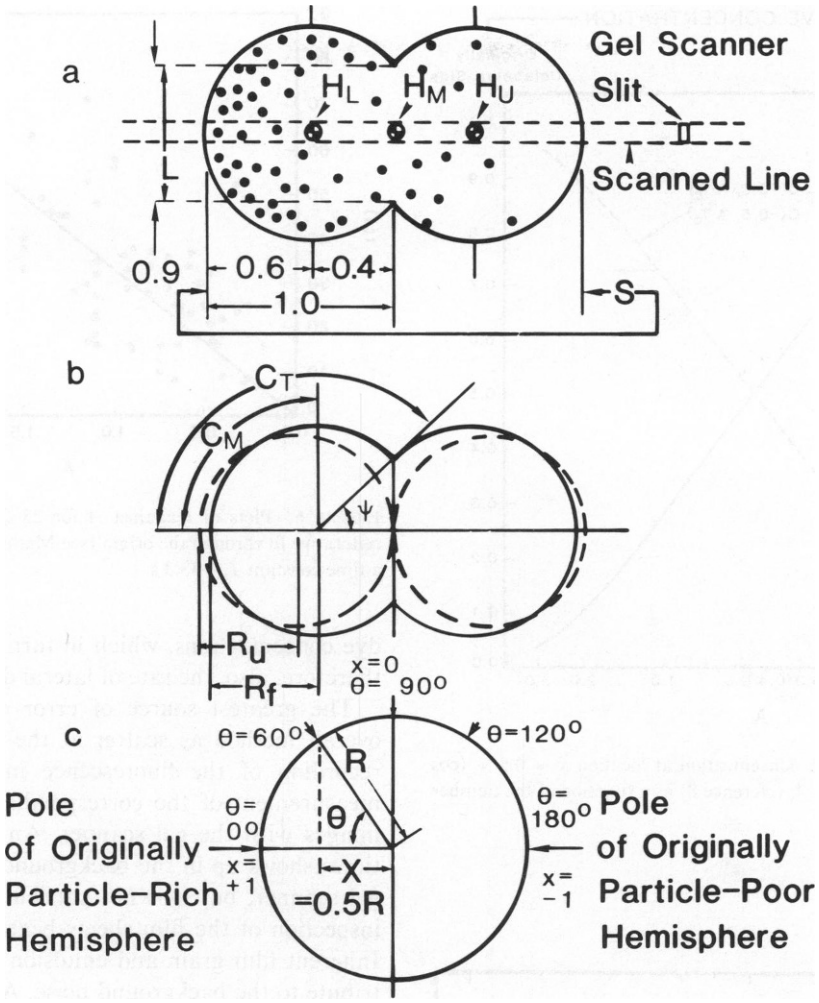

FIGURE 3 Determining the location on Huang's model that corresponds to location on hourglass-shaped fusion product membranes where fluorescence was measured. (*a*) Relative dimensions, in numbers, of an average fusion product were derived from actual measurements of dimensions S and L. The location on photographically recorded images where optical density was measured was four-tenths of the distance toward the pole from the plane of the lumen. (*b*) Angle ψ was calculated from the relative dimensions of the average fusion product according to ψ = arctan $[(L/2)/0.4]$ = arctan (0.45/0.4) = 48°. Circumferential distance, C_M, from the pole to the location on the average fusion product where the optical density measurement was made is thus a proportion of the total circumferential distance, C_T, from the pole to the plane of the lumen. The proportion is 90°/(180°–48°) = 0.68. Using the average fusion product relative dimensions it can be shown that if the area of two unfused spheres with radius R_u is conserved on fusion then the radius R_f of each component sphere in the hourglass fusion product will be $R_f = 1.09\ R_u$. (*c*) The location on Huang's model for diffusion on a spherical membrane that corresponds to the location where optical density measurements were made will thus be at $\theta = 0.68\ (90°) = 60°$. Also, $X = R \cos (60°) = 0.5\ R$, and corresponds to the convention in Huang's model (Fig. 4, reference 8). It can be shown from the relative dimensions of the average fusion product that the radius of a sphere having the area of two fused spheres, each with radius R_f, are related according to $R = 1.29\ R_f$.

FIGURE 2 Sequence of micrographs (*A–D*) of fluorescence moving from an originally labeled membrane (*left*) to an originally unlabeled membrane (*right*) after fusion and sequence of corresponding concentration gradients (*E–H*) associated with the micrographs. Concentration gradients were generated from the linear transmission of light (in arbitrary units) through the positive image on film from a rectangular light source scanned as shown in Fig. 3 *a*. time, t (s), after fusion; (*A, E*), 9; (*B, F*), 18; (*C, G*), 30; (*D, H*), 48.

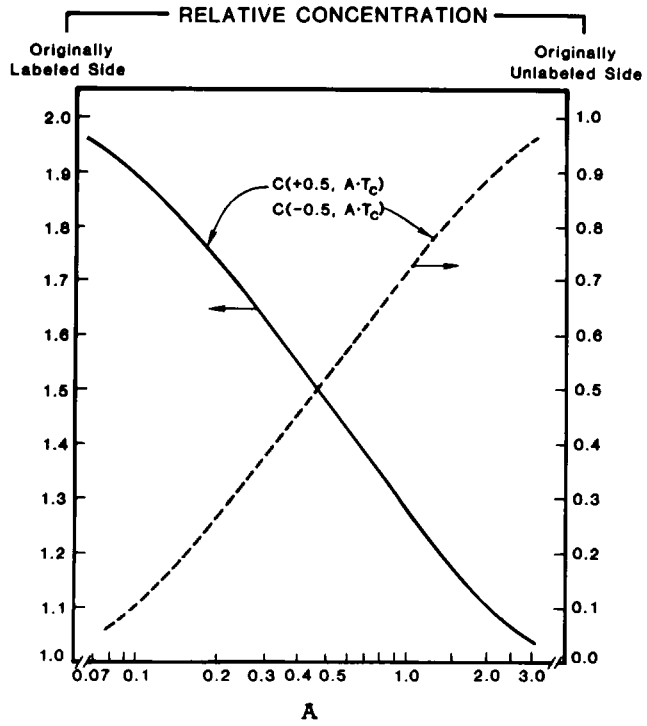

FIGURE 4 Plot of change in concentration at location $x = 0.5 = (\cos 60°)$, on Huang's model (Fig. 4, reference 8) as a function of the number A.

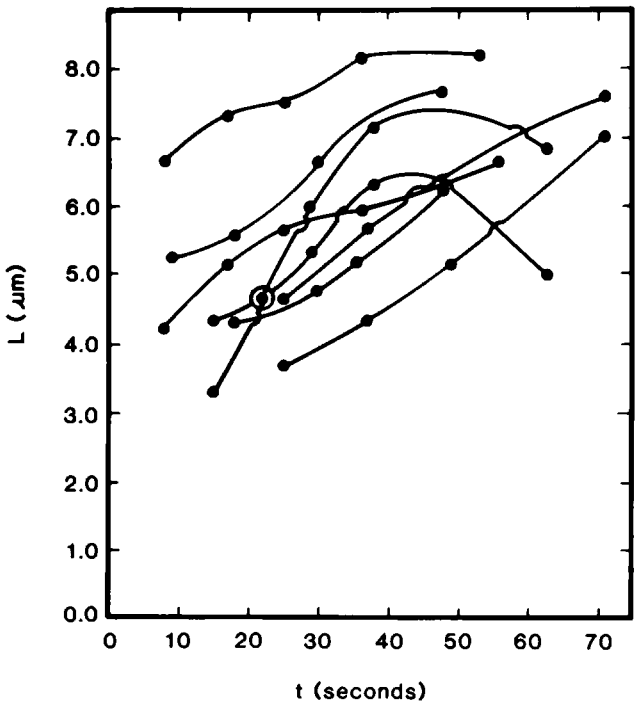

FIGURE 5 Lumen diameter, L, as function of time, t, after fusion for sequences of micrographs of individual fusion product membranes selected to illustrate wide variability in rates of increases.

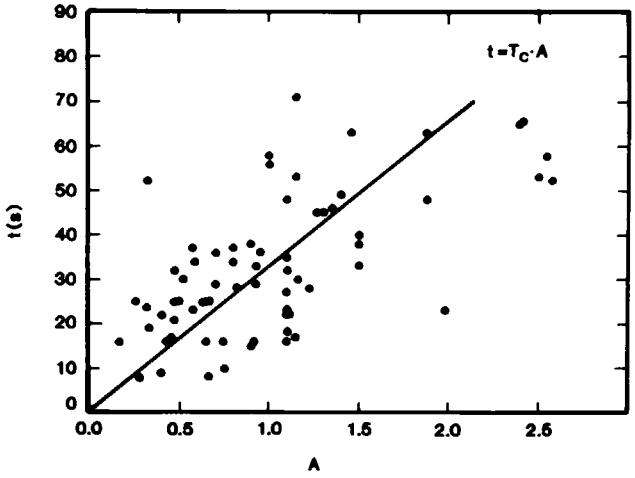

FIGURE 6 Plots of t against A for 23–25°C data. Straight line is a reiterative fit through the origin (see Methods). Solid line corresponds to a time constant $T = 33.3$ s.

dye concentrations, which in turn lower the gradient and therefore, also, the rate of lateral diffusion.

The greatest source of error enters the data of this overall method as scatter at the stages that include the recording of the fluorescence images on film and the measurement of the corresponding gradients from those images with the gel scanner. An anomalous drift sometimes shows up in the background in the curves from the gel scanner, but it is not particularly apparent by visual inspection of the film sheets bearing the positive images. Inherent film grain and emulsion heterogeneity also contribute to the background noise. A few fusion events have been seen that lead first to irregularly shaped hourglass fusion products, which rapidly become normal in time but may contribute some unsymmetrical lateral concentration gradients to the data pool.

Two important distinctions exist between the fusion approach and the conventional photobleaching approach to measuring lateral diffusion coefficients. First, the conventional photobleaching study involves the examination of fluorescence recovery inside a small spot area usually much smaller than the membrane, whereas in the fusion approach, the gradient extends over the entire length of the

TABLE I
LATERAL DIFFUSION COEFFICIENTS FOR DiI IN HUMAN ERYTHROCYTE MEMBRANES

Value ($\times 10^9$)		Reference
(23–25°C)	(35–37°C)	
cm^2/s		
3.8	8.1	This study
3*	5*	9
1.7	2.1	10
8.4	21.0	11

*Discoid ghost membranes.

membrane. Second, the bleaching event takes place rapidly and in a local area. The bleaching event is assumed to cause a significant change in the fluorescence of a large fraction of the labels without causing a change in the molecular structure of the labeled molecules which may either cause a change in mobility or effectively add a new species of diffusing molecule. The fusion approach does not depend on bleaching but, rather, is aided by the absence of it. This leaves only the question of whether the labeled molecule is a good model for lateral mobility of the unlabeled molecules in the host membrane. Ideally, the lateral diffusion coefficient should be independent of the method of measurement. Indeed, this appears to be the case when comparing our results with previously published photobleaching data.

Beyond the obviously greater simplicity of the instrumentation, the fusion appraoch to measuring lateral diffusion has some potential advantages when compared with conventional photobleaching. First, the fusion approach can more easily accommodate membrane systems in suspension—photobleaching usually depends on membranes immobilized on a substratum. Second, membranes that are close in size (e.g., mitochondrial inner membranes, platelets, vesicles, mycoplasmas, etc.) to the smallest photobleaching spot sizes available may be more easily studied using the fusion approach than by using the photobleaching approach if a labeled membrane and one or more unlabeled membranes are fused together to make longer diffusion gradients. Third, the fusion approach is potentially applicable to the measurement of the lateral diffusion of intramembrane particles from an intramembrane particle-rich membrane to an intramembrane particle-poor membrane using freeze-fracture electron microscopy. The last approach would eliminate the need for any exogenous or foreign molecule to be introduced into the membrane under study.

The expert technical assistance of Ms. Veena Kapoor and Mr. Christopher O. Conway is greatly appreciated.

Contribution No. 621 from the American Red Cross Laboratories. Supported in part by Biomedical Research Grant No. 5 SO RR05737.

Received for publication 20 April 1984 and in final form 29 October 1984.

Note Added in Proof: Koppel, D. E. (1984, *Biophys J.* 46:837–840) has developed a method by which our estimate of the lateral diffusion coefficient can be corrected so as to make an allowance for the doublet geometry of our fusion products.

REFERENCES

1. Frye, L. D., and M. Edidin. 1970. The rapid intermixing of cell surface antigens after formation of mouse-human heterokaryons. *J. Cell. Sci.* 7:319–335.
2. Edidin, M., and T. Wei. 1977. Diffusion rates of cell surface antigens of mouse-human heterokaryons. I. Analysis of the population. *J. Cell. Biol.* 75:475–482.
3. Fowler, V., and D. Branton. 1977. Lateral mobility of human erythrocyte integral membrane proteins. *Nature (Lond.).* 286:23–26.
4. Schindler, M., D. E. Koppel, and M. P. Sheetz. 1980. Modulation of membrane protein lateral mobility of polyphosphates and polyamines. *Proc. Natl. Acad. Sci. USA.* 77:1457–1461.
5. Zimmerman, U. 1982. Electric field-mediated fusion and related electrical phenomena. *Biochim. Biophys. Acta.* 694:227–277.
6. Zimmerman, U., and J. Vienken. 1982. Electric field-induced cell-to-cell fusion. *J. Membr. Biol.* 67:165–182.
7. Sowers, A. E. 1984. The lateral diffusion of DiI from a labeled membrane to an unlabeled membrane following electric field induced fusion: A new quantitative technique. *Biophys. J.* 45(2, Pt. 2):331*a*. (Abstr.)
8. Huang, H.-W. 1973. Mobility and diffusion in the plane of cell membrane. *J. Theor. Biol.* 40:11–17.
9. Kapitza, H.-G., and E. Sackmann. 1980. Local measurement of lateral motion in erythrocyte membranes by photobleaching technique. *Biochim. Biophys. Acta.* 595:56–64.
10. Thompson, N. L., and D. Axelrod. 1980. Reduced lateral mobility of a fluorescent lipid probe in cholesterol-depleted erythrocyte membrane. *Biochim. Biophys. Acta.* 597:155–165.
11. Bloom, J. A., and W. W. Webb. 1983. Lipid diffusibility in the intact erythrocyte membrane. *Biophys. J.* 42:295–305.